

Supporting Information

Polarization-Directed Growth of Single-Crystalline Silicon Nanostructures

Jin Hu¹, Jin Qin¹, and Zhikun Liu^{1,*}

¹ School of Mechanical Engineering, Shanghai Jiao Tong University, Shanghai
200240, China

* Author to whom correspondence should be addressed: liuzhikun@sjtu.edu.cn

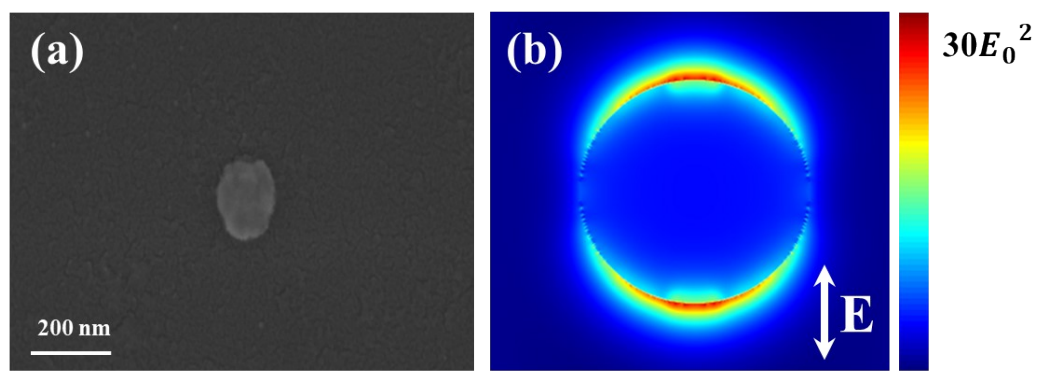


Figure S1. SEM image of Ag nanoparticle and FDTD simulated localized surface plasmon effects.
(a) Ag nanoparticles fabricated on an alumina substrate by electron-beam lithography. (b) Simulated near-field distribution at a plane 2 nm above the substrate, showing the localized surface plasmon enhancement of the Ag nanoparticles under illumination with a wavelength of 343 nm, obtained using FDTD simulations.

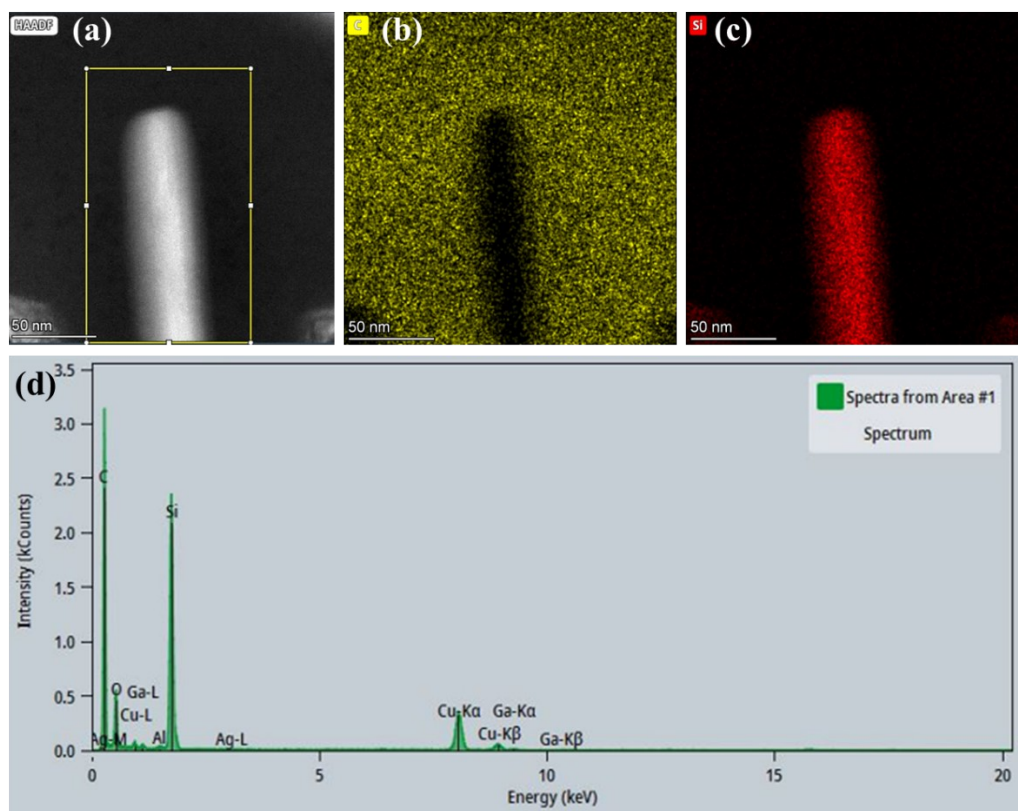


Figure S2. Elemental analysis of the silicon nanostructures. (a–c) HAADF-STEM image and corresponding elemental mapping of the silicon nanostructures. (d) EDS spectrum of the analyzed region. The absence of the Ag-L peak in the X-ray spectrum indicates that no silver element was detected in the silicon nanostructures.

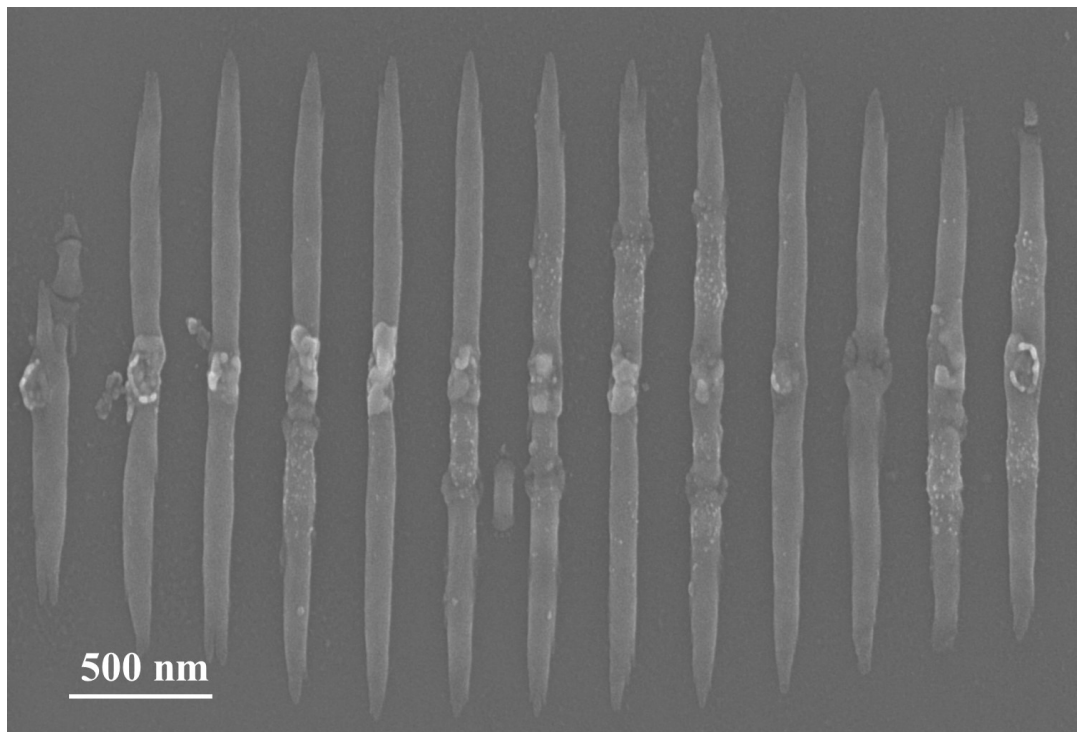


Figure S3. SEM image of silicon nanostructures grown on Fe nanoparticles, aligned with the laser polarization.

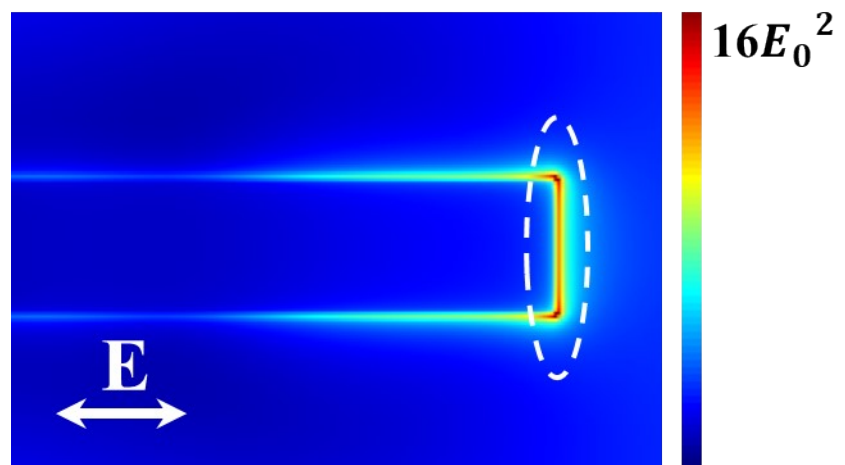


Figure S4. Simulated near-field distribution at the silicon growth front for growth aligned with the polarization direction.

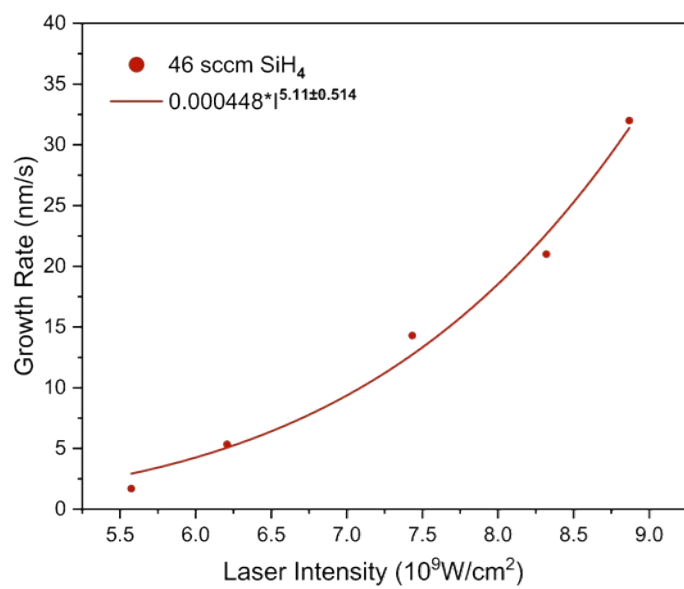


Figure S5. Growth rate as a function of the peak intensity of incident laser irradiation at 515 nm.

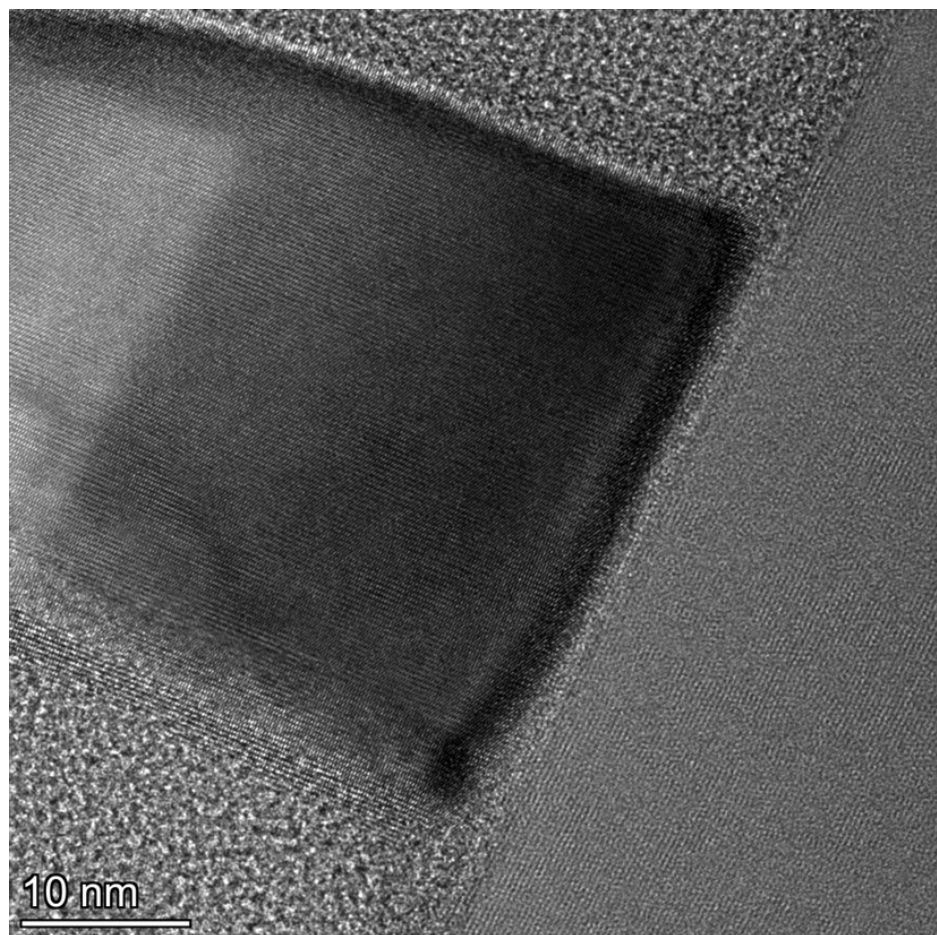


Figure S6. HRTEM image of silicon nanostructures grown on a silicon substrate. The inconsistency in lattice orientations confirms a non-epitaxial growth mode.

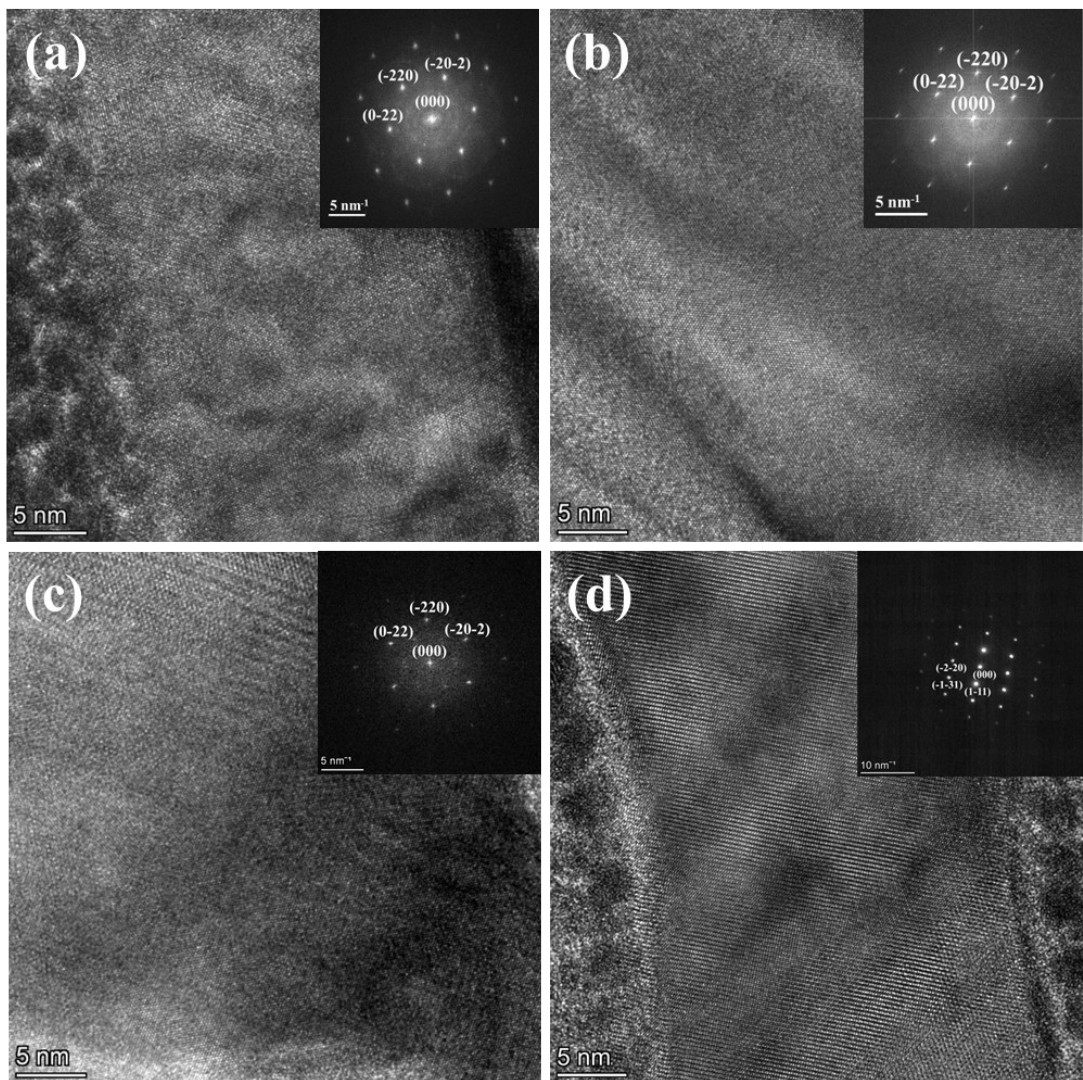


Figure S7. Cross-sectional TEM and corresponding FFT images of silicon nanostructures taken perpendicular to the growth (polarization) direction. (a–c) Zone axis $[-111]$; (d) Zone axis $[-112]$.

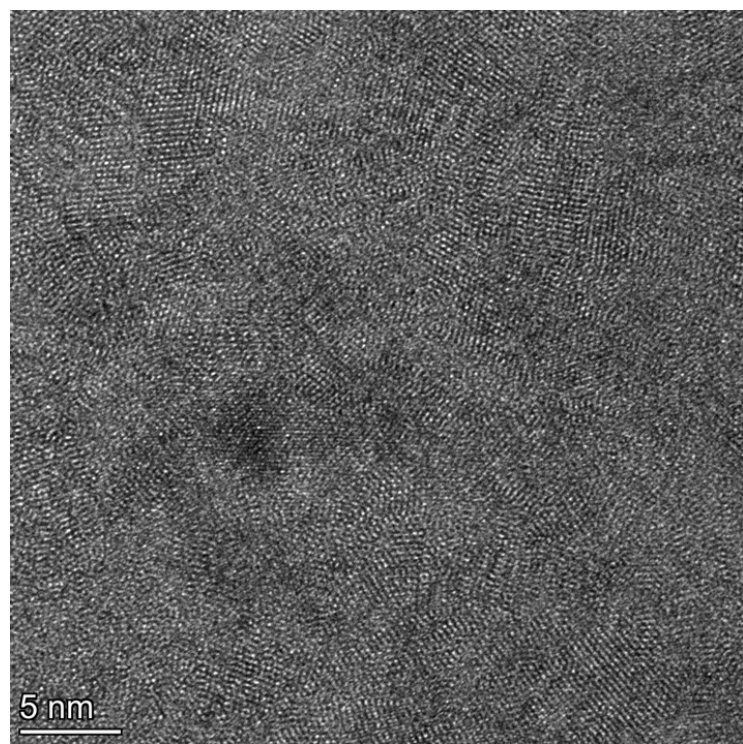


Figure S8. High-resolution transmission electron microscopy (HRTEM) image of silicon nanostructures grown under 515 nm wavelength laser irradiation at a relatively low intensity ($5 \times 10^9 \text{ W m}^{-2}$).

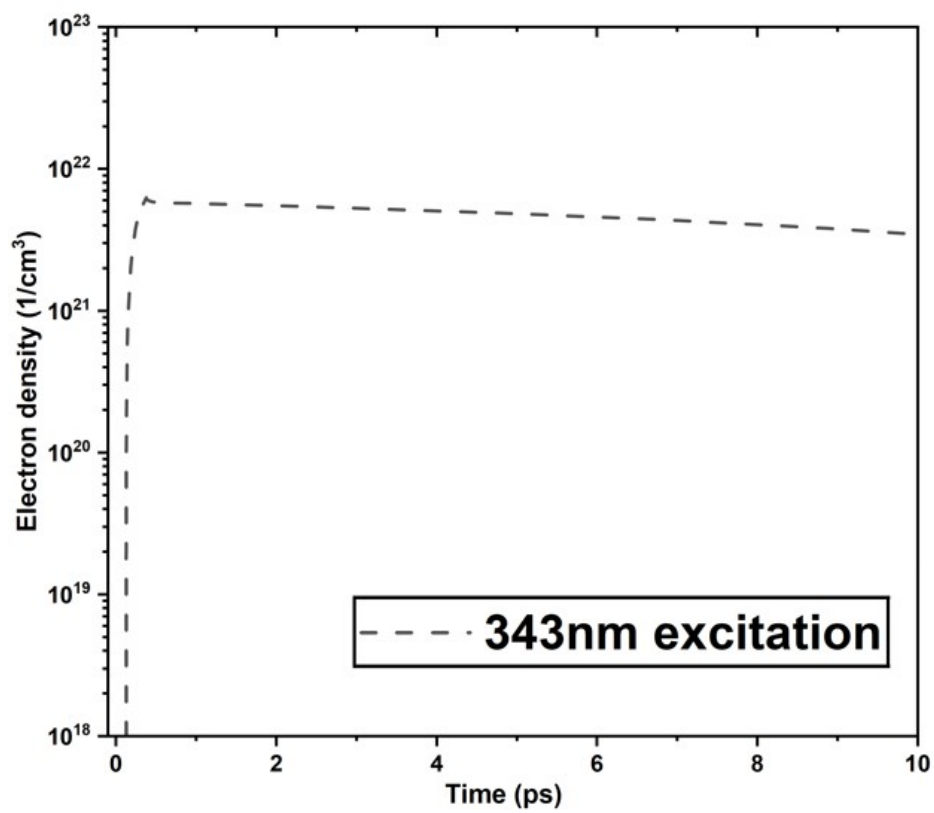


Figure S9. Carrier density evolution on the surface of silicon nanostructures under 343 nm laser irradiation, calculated using the two-temperature model.

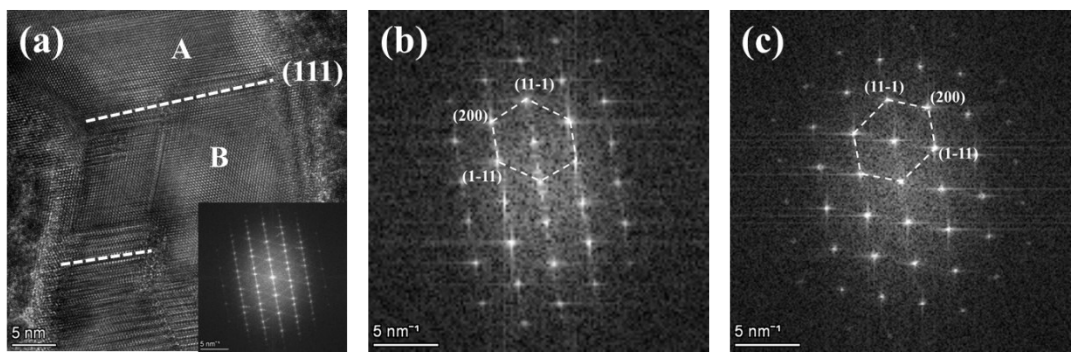


Figure S10. TEM characterization of silicon nanostructures grown on a silicon substrate.
(a) High-resolution TEM image of a twin boundary within the silicon nanostructures and the corresponding selected area electron diffraction (SAED) pattern. The zone axis is [110].
(b–c) SAED patterns of adjacent twin regions A and B.